SIAM J. NUMER. ANAL.
Vol. 40, No. 4, pp. 1446–1474

DYNAMIC ITERATION USING REDUCED ORDER MODELS: A METHOD FOR SIMULATION OF LARGE SCALE MODULAR SYSTEMS*

MURUHAN RATHINAM† AND LINDA R. PETZOLD†

Abstract. We describe a new iterative method, dynamic iteration using reduced order models (DIRM), for simulation of large scale modular systems using reduced order models that preserve the interconnection structure. This method may be compared to the waveform relaxation technique; however, unlike DIRM, waveform relaxation does not take advantage of model reduction techniques. The DIRM method involves simulating in turn each subsystem connected to model reduced versions of the other subsystems. The data from this simulation is then used to update the reduced model for that particular subsystem. We provide analytical results on convergence and accuracy of the DIRM method as well as numerical examples that demonstrate the success of DIRM and verify the analysis.

Key words. large scale systems, model reduction, dynamic iteration, proper orthogonal decomposition

AMS subject classifications. 65L99, 65M20

PII. S0036142901390494

1. Introduction.

Very large scale systems of differential and differential algebraic equations such as the U.S. power grid, very large scale integrated (VLSI) circuits, chemical reactors, and weather systems present challenges in computing. Usually such large scale systems consist of many interacting subsystems, which may in some problems be governed by very different physical laws. On such systems conventional methods of direct numerical integration of the full system may not be feasible without massive computing resources.

An iterative approach known as *waveform relaxation* (WR), where smaller subsystems are simulated separately and then the couplings are accounted for through iteration, was developed by researchers for the simulation of VLSI circuits. See Lelarasmee, Ruehli, and Sangiovanni-Vincentelli [7], Miekkala and Nevanlinna [9], and Miekkala [8] for details. The WR method is a form of *dynamic iteration* in the sense that the variable being iterated is a function (the entire solution waveform for a given time interval) and not a vector. This method has subsequently been applied by researchers to PDEs of parabolic and hyperbolic types [2]. Such a modular approach in principle has the advantage that it facilitates parallel computation, exploits the multirate nature of some problems, and offers the potential of using different numerical techniques for different subsystems. However, the WR technique has not become the mainstay in application areas. This is primarily due to the poor convergence properties of WR.

Another way to deal with models that are too complex is via model reduction. Several model reduction techniques have been studied by researchers in various fields. *Balanced truncation* has been studied by the control community (see Zhou and Doyle [15] and Lall, Marsden, and Glavaski [6], for instance), *proper orthogonal decomposition* (POD) has been applied in the study of turbulence (see Holmes, Lumley, and

*Received by the editors June 7, 2001; accepted for publication (in revised form) March 28, 2002; published electronically October 23, 2002. A preliminary version of this article appeared in *Proceedings of the IEEE Control and Decision Conference*, Sydney, Australia, 2000. This research was supported in part by grants EPRI WO-8333-06, NSF/KDI ATM-9873133, and NSF ACI-0086061.
http://www.siam.org/journals/sinum/40-4/39049.html

†Computational Science and Engineering, University of California, Santa Barbara, CA 93106 (muruhan@engineering.ucsb.edu, petzold@engineering.ucsb.edu).

Berkooz [5]), cascading failures in power grids (Parrilo et al. [11]), and control of compressors (Glavaski, Marsden, and Murray [3]), etc., and *selective modal analysis* has been developed by researchers in the electrical power field (Perèz-Arriaga et al. [12]), to name a few.

In this paper we present a method that combines the idea of dynamic iteration with the use of reduced order models. Our method also seeks to remedy some of the shortcomings of WR. Our approach, termed dynamic iteration using reduced order models (DIRM), involves simulation of each subsystem in turn while it is connected to reduced order models of the rest of the subsystems. The simulation results are then used to update the reduced order model for that particular subsystem. If the reduced order models are small enough, then the combination of an unreduced subsystem with the rest of the reduced subsystems results in a system small enough not to pose insurmountable computational difficulties. In principle any model reduction method that uses data from trajectories could be used in this iteration. In this paper we use POD (also known as *Karhunen–Loève decomposition*) for the model reduction.

Even though theoretically the WR method has good asymptotic convergence, in practice there may be large initial overheads. For example, consider a one-dimensional (1D) PDE with the spatial domain divided into 10 subsystems of adjacent regions. It will take nine iterations before the first subsystem "sees" the last subsystem. In the DIRM method, by contrast, every subsystem is connected to all other (reduced versions of) subsystems, and one may not expect such overheads. This is possible only because of the fact that DIRM incorporates reduced order models.

This paper is organized as follows. In section 2 we review the POD method of model reduction and comment on its application to modular systems. In section 3 we describe DIRM in detail and also provide a brief account of the WR technique. In section 4 we provide an analysis of the DIRM method as applied to a linear time invariant system consisting of two subsystems and present results on the accuracy and convergence behavior of DIRM. Section 5 describes several numerical examples. These include a nonlinear power grid simulation and some reaction diffusion problems described by PDEs, with comparison to WR. We also give some examples highlighting certain special cases, which include situations where DIRM has difficulty converging as predicted by the analysis, and show how to modify DIRM to fix this problem. Finally, in section 6 we present conclusions and discuss future research.

2. Model reduction using POD. The POD technique for model reduction consists of first finding a subspace in the full phase space of a given dynamical system and then constructing an approximating dynamical system in that subspace. The original dynamical system may be nonlinear, and in that case the resulting lower dimensional model will also typically be nonlinear.

2.1. POD. POD, also known as Karhunen–Loève decomposition or principal component analysis, provides a method for finding the best approximating subspace to a given set of data. Originally POD was used as a data representation technique. For model reduction of dynamical systems POD may be used on data points obtained from system trajectories obtained via experiments, numerical simulations, or analytical derivations. For more information see Rathinam and Petzold [13], Holmes, Lumley, and Berkooz [5], Moore [10], Lall, Marsden, and Glavaski [6], Glavaski, Marsden, and Murray [3], and references therein.

Given a set of data points $x^{(\alpha)} \in \mathbb{R}^n$, POD seeks a subspace $S \subset \mathbb{R}^n$ so that the total square distance

$$D = \sum_{\alpha=1}^{N} \left\| x^{(\alpha)} - \rho_S x^{(\alpha)} \right\|^2,$$

where ρ_S is the orthogonal projection onto the subspace S, is minimized. The norm considered is the 2-norm. (Thus we assume that the phase space comes equipped with a notion of inner product.) The solution to this problem may be stated in terms of the *correlation matrix* defined by

$$R = \sum_{\alpha=1}^{N} x^{(\alpha)} \left(x^{(\alpha)} \right)^T.$$

Note that R is $n \times n$ and symmetric positive semidefinite. Let $\lambda_1 \geq \lambda_2 \cdots \geq \lambda_n \geq 0$ be the ordered eigenvalues of R. Then the minimum value of D over all $k(\leq n)$ dimensional subspaces S is given by $\sum_{j=k+1}^{n} \lambda_j$ [5]. In addition, the S that minimizes D is the invariant subspace corresponding to the eigenvalues $\lambda_1, \ldots, \lambda_k$. In practice one need not compute R. Instead, it is efficient to use the $n \times N$ matrix X whose columns are $x^{(\alpha)}$. Then $\sqrt{\lambda_1}, \ldots, \sqrt{\lambda_n}$ are the singular values of X (assuming $n \leq N$), and S is the span of the left singular vectors of X corresponding to k the largest singular values. Note that $R = XX^T$.

Often it may be best to find an affine subspace as opposed to a linear subspace. This requires first to find the mean value of the data points

$$\bar{x} = \frac{1}{N} \sum_{\alpha=1}^{N} x^{(\alpha)}$$

and then construct the *covariance matrix* $\bar{R}$ given by

$$\bar{R} = \sum_{\alpha=1}^{N} \left(x^{(\alpha)} - \bar{x} \right) \left(x^{(\alpha)} - \bar{x} \right)^T.$$

Let S_0 be the invariant subspace of the k largest eigenvalues of $\bar{R}$. Then the best approximating affine subspace S passes through $\bar{x}$ and is obtained by shifting S_0 by $\bar{x}$. Algebraically the projection onto the subspace S is given by

$$z = \rho(x - \bar{x}), \tag{2.1}$$

where $z \in \mathbb{R}^k$ are coordinates in the subspace S, $x \in \mathbb{R}^n$ are coordinates in the original coordinate system in $\mathbb{R}^n$, and the matrix ρ of the projection consists of row vectors ϕ_i^T $(i = 1, \ldots, k)$, where ϕ_i are the unit eigenvectors corresponding to the largest k eigenvalues of $\bar{R}$. Note that given any point $p \in S$ with coordinates $z \in \mathbb{R}^k$ the coordinates $x \in \mathbb{R}^n$ of the same point in the original coordinate system are given by

$$x = \rho^T z + \bar{x}.$$

2.2. Galerkin projection. Having found the approximating subspace for our system data, our next task is to construct a vector-field on this subspace that represents the reduced order model. This procedure is known as Galerkin projection and has been widely used in reducing PDEs to ODEs by projecting onto appropriate basis functions that describe the spatial variations in the solution. The procedure is applicable to any subspace; the subspace need not be obtained from the POD method. See [5] for more details.

Suppose the original dynamical system in $\mathbb{R}^n$ is given by a vector-field f,

$$\dot{x} = f(x,t).$$

Let $S \subset \mathbb{R}^n$ be the best k dimensional approximating affine subspace with projection given by (2.1). A vector-field f_a in the subspace S is constructed by the following rule: for any point $p \in S$ compute the vector-field $f(p,t)$ and take the projection $\rho f(p,t)$ onto the subspace S to be the value of $f_a(p,t)$. If z are the subspace coordinates of p, then $f_a(z,t) = \rho f(\rho^T z + \bar{x}, t)$. Thus we obtain the following reduced model:

$$\dot{z} = f_a(z,t) = \rho f(\rho^T z + \bar{x}, t). \tag{2.2}$$

If we are solving an initial value problem with $x(0) = x_0$, then in the reduced model one has the initial condition $z(0) = z_0$, where

$$z_0 = \rho(x_0 - \bar{x}).$$

Hence the approximating solution $\hat{x}(t)$ in the original coordinates in $\mathbb{R}^n$ is given by

$$\hat{x}(t) = \rho^T z(t) + \bar{x}.$$

From the above it is easy to see that the approximating solution $\hat{x}(t)$ is the solution to the following initial value problem:

$$\dot{\hat{x}} = Pf(\hat{x},t), \qquad \hat{x}(0) = \hat{x}_0 = P(x_0 - \bar{x}) + \bar{x}, \tag{2.3}$$

where $P = \rho^T \rho \in \mathbb{R}^{n \times n}$ is the matrix of the projection expressed in the original coordinate system in $\mathbb{R}^n$. Also note that $\hat{x}_0$ is just the projection of x_0 onto the affine subspace S.

2.3. Modular model reduction. In this paper *modular system* shall mean any system expressed in the form

$$\dot{x}_i = f_i(x_1, \ldots, x_m, t), \qquad i = 1, \ldots, m. \tag{2.4}$$

Note that any system $\dot{x} = f(x,t)$ can be written in this form. All that is involved is a partitioning of the states $x = (x_1, \ldots, x_m)$, where $x_i \in \mathbb{R}^{n_i}$ are vectors. This partitioning may arise naturally from the physical interpretation of the system, as in the power grid example presented later, or may be introduced according to some optimal criteria for the simulation problem at hand. In this paper we consider situations where the overall system is very large; hence we modularize the system by breaking it into manageable smaller parts. The POD method can be made to "respect" the partitioning by forming separate covariance matrices for each of the subsystem states $x_i \in \mathbb{R}^{n_i}$,

$$\bar{R}_i = \sum_{\alpha=1}^{N} \left(x_i^{(\alpha)} - \bar{x}_i \right) \left(x_i^{(\alpha)} - \bar{x}_i \right)^T,$$

and computing separate projections $\rho_i \in \mathbb{R}^{k_i \times n_i}$ that operate within the state space of a subsystem. Thus the reduced model will be

$$\dot{z}_i = \rho_i f_i(\rho_1^T z_1 + \bar{x}_1, \ldots, \rho_m^T z_m + \bar{x}_m, t), \qquad i = 1, \ldots, m.$$

3. DIRM. In this section we describe the DIRM method of simulating a large scale modular system of the form (2.4). We first describe the WR method in order to put our method in context.

The basic idea behind WR as applied to system (2.4) may be explained as follows. Start with an initial approximation for solutions of each of the subsystem trajectories: $x_1^{(0)}(t), \ldots, x_m^{(0)}(t)$. At the kth iteration, simulate each subsystem separately:

$$\dot{x}_i^{(k)} = f_i(x_1^{(k-1)}(t), \ldots, x_{i-1}^{(k-1)}(t), x_i^{(k)}, x_{i+1}^{(k-1)}(t), \ldots, x_m^{(k-1)}(t), t), \quad i = 1, \ldots, m.$$

This is a simplified explanation of the method. For a detailed exposition and analysis we refer to [7], [9], and [8]. It has been shown that this iteration converges for ODE systems in finite interval simulations under some mild conditions. However, WR may suffer from slow convergence. Overlapping techniques are often used to speed up the convergence [8].

The DIRM method also simulates each subsystem in turn, but not in isolation. Instead, the unreduced model of the subsystem is connected to reduced order models of the other subsystems. If the reduced order models are small enough, then the overall size of the resulting system is still of manageable dimensions. Consider the modular system (2.4) with initial conditions $x_i(0) = x_{i,0}$ and suppose we are interested in a simulation interval $[0, T]$. The DIRM method is described as follows.

Start with some initial reduced model for each subsystem. In the POD approach a reduced model for subsystem i is characterized by the projection matrix ρ_i and the mean data value $\bar{x}_i$. Let the initial reduced models be $(\rho_i^{(0)}, \bar{x}_i^{(0)})$. One way to generate these is to simulate each subsystem in isolation (in the given interval), setting the states of the other subsystems to some constant values, for instance, the initial conditions. In other words, simulate the following equations:

$$\dot{x}_i = f_i(x_{1,0}, x_{2,0}, \ldots, x_{i-1,0}, x_i, x_{i+1,0}, \ldots, x_{m,0}, t), \qquad i = 1, \ldots, m,$$

with initial conditions $x_i = x_{i,0}$. The resulting solutions $x_i(t)$ may be used to compute the covariance matrices $\bar{R}_i$:

$$\begin{aligned} \bar{x}_i &= \frac{1}{T} \int_0^T x_i(t) dt, \\ \bar{R}_i &= \int_0^T (x_i(t) - \bar{x}_i)(x_i(t) - \bar{x}_i)^T dt. \end{aligned} \tag{3.1}$$

At the jth step in the iteration we have the reduced models from the previous step $(\rho_i^{(j-1)}, \bar{x}_i^{(j-1)})$. We also have the trajectories $x_i^{(j-1)}(t), t \in [0, T]$, which were used in constructing these reduced models. Now for $i = 1, \ldots, m$ connect the unreduced subsystem i with the reduced versions of all other subsystems and simulate the resulting system

$$\begin{aligned} \dot{x}_i &= f_i(X, t), \\ \dot{z}_l &= \rho_l^{(j-1)} f_l(X, t), \qquad l = 1, \ldots, i-1, i+1, \ldots, m, \end{aligned} \tag{3.2}$$

where X is the following list of vector arguments:

$$X = \left(\rho_1^{(j-1)}\right)^T z_1 + \bar{x}_1^{(j-1)}, \ldots, \left(\rho_{i-1}^{(j-1)}\right)^T z_{i-1} + \bar{x}_{i-1}^{(j-1)}, \\ x_i, \left(\rho_{i+1}^{(j-1)}\right)^T z_{i+1} + \bar{x}_{i+1}^{(j-1)}, \ldots, \left(\rho_m^{(j-1)}\right)^T z_m + \bar{x}_m^{(j-1)}.$$

Use the resulting trajectory for the ith subsystem $x_i^{(j)}(t)$ to compute an updated reduced order model for the ith subsystem $(\rho_i^{(j)}, \bar{x}_i^{(j)})$. The iteration is terminated when

$$\sup_{t\in[0,T]} \left\{ \|x_i^{(j)}(t) - x_i^{(j-1)}(t)\| \right\} \leq tol, \qquad i = 1, \ldots, m, \tag{3.3}$$

where *tol* is some specified tolerance.

Remark 3.1. In (3.2) the trajectories $z_l^{(j)}(t)$ correspond to reduced models, while the trajectory $x_i^{(j)}(t)$ corresponds to the full model. In situations when the coupling between subsystems is "weak," $x_i^{(j)}(t)$ will be more accurate than $z_l^{(j)}(t)$. Since the reduced models are computed directly from $x_i^{(j)}(t)$, the simulation for the next iteration $j+1$ is directly affected by $x_i^{(j)}(t)$ and only indirectly by $z_l^{(j)}(t)$. This helps keep the effect of errors due to model reduction small. Also note that the final solution comes directly from $x_i^{(j)}(t)$, and the $z_l^{(j)}(t)$ enter only indirectly.

For any technique involving reduced order models, accuracy is an important issue. Since reduced order models are computed from the trajectories obtained from the given initial value problem, when the coupling dynamics is not very strong the situation for DIRM is reasonably close to the circumstances under which the accuracy of the POD method could be expected to be as good as possible as indicated by the error analysis of POD in [13].

We have observed from various examples, linear and nonlinear, that the DIRM method generally converges. We have also found examples where it fails to converge, but on those occasions breaking up the time interval $[0, T]$ into smaller ones $[t_i, t_{i+1}]$, $i = 0, \ldots M-1$, where $t_0 = 0$ and $t_M = T$ and running the algorithm successively in each interval achieves convergence. It is known that WR also converges better when the interval length is smaller. However, of course there is an optimal length beyond which making the intervals smaller results in higher computational effort.

Remark 3.2. The method of model reduction we use in this paper is POD, but in the overall iteration of DIRM one could in principle replace POD with any model reduction scheme that depends on simulation data. (Methods such as balanced truncation in their original form cannot be used, since they depend only on the model and not on a given set of system trajectories.)

4. Analysis for linear time invariant systems with two subsystems. The iteration operator associated with DIRM is nonlinear even if the system of ODEs is linear. This significantly complicates the convergence analysis of DIRM. In this section we provide an analysis of the DIRM method for linear time invariant systems consisting of two subsystems. We also assume that in the model reduction via POD we fit the best approximating linear subspace instead of the more general method of fitting the best approximating affine subspace. Although these assumptions are somewhat restrictive, the purpose of the analysis is to provide qualitative results rather than sharp estimates of convergence rates.

4.1. Description of Jacobi DIRM iteration operator for two subsystems. Throughout the rest of section 4 we will be concerned with the case of two subsystems each of dimension n unless stated otherwise. Suppose that the system consists of states $x = (x_1, x_2)$ with $x_i \in \mathbb{R}^n$ for $i = 1, 2$, and that the system equations are given by

$$\begin{aligned} \dot{x}_1 &= A_1 x_1 + A_{12} x_2, \\ \dot{x}_2 &= A_{21} x_1 + A_2 x_2, \\ x_1(0) &= x_{10}, \qquad x_2(0) = x_{20}, \end{aligned} \tag{4.1}$$

and that we are interested in the finite simulation interval $[0, T]$. We shall also use the compact notation $\dot{x} = Ax,\ x(0) = x_0$ to denote the same system. We start with some approximate solution $x^{(0)}(t)$ of the system as the initial (zeroth) iterate. For instance we may use the solution of the decoupled systems given by $x^{(0)} = (x_1^{(0)}, x_2^{(0)})$ which satisfies $\dot{x}_1^{(0)} = A_1 x_1^{(0)},\ x_1^{(0)}(0) = x_{10}$ and $\dot{x}_2^{(0)} = A_2 x_2^{(0)},\ x_2^{(0)}(0) = x_{20}$. Another approach may be to use some reduced order model solution as $x^{(0)}$. Our analysis does not depend on this initial choice.

Suppose we have trajectory $x^{(\alpha)}$ at the αth iteration. Then we find best approximating $k(\leq n)$ dimensional subspaces in $\mathbb{R}^n$ (k is fixed throughout the iterations) and the corresponding orthogonal projections $P_1^{(\alpha)}$ and $P_2^{(\alpha)}$ (both are $n \times n$ matrices) for the trajectories $x_1^{(\alpha)}$ and $x_2^{(\alpha)}$, respectively. The next iterate $x^{(\alpha+1)}$ is obtained by forming partially reduced models. We combine unreduced system 1 with reduced system 2 to obtain $x_1^{(\alpha+1)}$ and similarly for $x_2^{(\alpha+1)}$. Then we find the projections $P_1^{(\alpha+1)}$ and $P_2^{(\alpha+1)}$ corresponding to $x_1^{(\alpha+1)}$ and $x_2^{(\alpha+1)}$. Thus if

$$P^{(\alpha)} = \begin{bmatrix} P_1^{(\alpha)} & 0_{n\times n} \\ 0_{n\times n} & P_2^{(\alpha)} \end{bmatrix}$$

is the combined projection at the α th iteration, then $x^{(\alpha+1)}$ is given by

$$\begin{aligned} \dot{x}_1^{(\alpha+1)} &= A_1 x_1^{(\alpha+1)} + A_{12} \hat{x}_2^{(\alpha+1)}, \\ \dot{\hat{x}}_2^{(\alpha+1)} &= P_2^{(\alpha)} A_{21} x_1^{(\alpha+1)} + P_2^{(\alpha)} A_2 \hat{x}_2^{(\alpha+1)}, \\ x_1^{(\alpha+1)}(0) &= x_{10}, \qquad \hat{x}_2^{(\alpha+1)}(0) = P_2^{(\alpha)} x_{20} \end{aligned} \tag{4.2}$$

and

$$\begin{aligned} \dot{\hat{x}}_1^{(\alpha+1)} &= P_1^{(\alpha)} A_1 \hat{x}_1^{(\alpha+1)} + P_1^{(\alpha)} A_{12} x_2^{(\alpha+1)}, \\ \dot{x}_2^{(\alpha+1)} &= A_{21} \hat{x}_1^{(\alpha+1)} + A_2 x_2^{(\alpha+1)}, \\ \hat{x}_1^{(\alpha+1)}(0) &= P_1^{(\alpha)} x_{10}, \qquad x_2^{(\alpha+1)}(0) = x_{20}. \end{aligned} \tag{4.3}$$

We can rewrite the above equations more compactly as

$$\begin{aligned} \dot{x}^{(\alpha+1)} &= A_d x^{(\alpha+1)} + A_o \hat{x}^{(\alpha+1)}, \\ \dot{\hat{x}}^{(\alpha+1)} &= P^{(\alpha)} A_o x^{(\alpha+1)} + P^{(\alpha)} A_d \hat{x}^{(\alpha+1)}, \\ x^{(\alpha+1)}(0) &= x_0, \qquad \hat{x}^{(\alpha+1)}(0) = P^{(\alpha)} x_0, \end{aligned} \tag{4.4}$$

where

$$P^{(\alpha)} = \begin{bmatrix} P_1^{(\alpha)} & 0_{n\times n} \\ 0_{n\times n} & P_2^{(\alpha)} \end{bmatrix}, \tag{4.5}$$

$$A_d = \begin{bmatrix} A_1 & 0_{n\times n} \\ 0_{n\times n} & A_2 \end{bmatrix}, \tag{4.6}$$

and

$$A_o = \begin{bmatrix} 0_{n\times n} & A_{12} \\ A_{21} & 0_{n\times n} \end{bmatrix}. \tag{4.7}$$

Thus $A = A_d + A_o$.

Define the iteration operator $\mathcal{I} : \mathcal{L}_2([0,T],\mathbb{R}^{2n}) \to \mathcal{L}_2([0,T],\mathbb{R}^{2n})$ as the one that maps $x^{(\alpha)}$ to $x^{(\alpha+1)}$. We are interested in the fixed points of this operator and their stability. It must be noted that $\mathcal{I}$ is essentially nonlinear and is the composition of two operators $\mathcal{I} = \mathcal{S} \circ \mathcal{R}$. Here $\mathcal{R} : \mathcal{L}_2([0,T],\mathbb{R}^{2n}) \to \mathcal{P}^2$ is the operator that maps $x^{(\alpha)}$ to $P^{(\alpha)} \in \mathcal{P}^2$, where $\mathcal{P} \subset \mathbb{R}^{n\times n}$ is the manifold of rank $k \le n$ orthogonal projections, and $\mathcal{S} : \mathcal{P}^2 \to \mathcal{L}_2([0,T],\mathbb{R}^{2n})$ maps $P^{(\alpha)}$ to $x^{(\alpha+1)}$ by (4.4). Let $X \in \mathcal{L}_2([0,T],\mathbb{R}^{2n})$ be the true solution of the original system of equations,

$$\dot{X} = AX, \qquad X(0) = x_0.$$

Let $x^* \in \mathcal{L}_2([0,T],\mathbb{R}^{2n})$ be any fixed point of $\mathcal{I}$, i.e., $\mathcal{I}x^* = x^*$. We would like x^* to be a good approximation for X. Our analysis will provide an upper bound on $\|x^* - X\|$. (All function norms are assumed to be 2-norms unless stated otherwise.) We shall show that the error depends on the norm of A_o (the off-diagonal part), the POD projection error $\|x^* - P^*x^*\|$, and the growth/decay properties of e^{At} in the time interval T.

Since $\mathcal{I}$ is nonlinear it is in general difficult to know if and how many fixed points exist. It is also difficult to determine whether $\mathcal{I}$ is globally contractive. In fact $\mathcal{I}$ is ill-defined for some trajectories x; this occurs when there are many k dimensional subspaces that best fit x in the least-square sense. However, it is clear that when A_o is the zero matrix, i.e., when the systems are decoupled, the iterations will converge after one step, and in addition there is only one fixed point. Under mild regularity conditions it can be shown that this fixed point will persist for nontrivial A_o, with $\|A_o\|$ small enough, and that this fixed point will be stable. We will provide an analysis that estimates the rate of convergence based on the linearization of $\mathcal{I}$ at a fixed point x^*. We will show that the convergence rate depends on $\|A_o\|$, norms of the exponentials of A and some related matrices, the interval length T, the error $\|x^* - P^*x^*\|$, as well as on the sensitivity of P to perturbations in x at the fixed point (x^*, P^*) which can be related to the eigenvalues of the correlation matrix of the fixed point trajectory x^*.

The rest of the subsections are organized as follows. In section 4.2 we summarize all the important results of our analysis up front. In section 4.3 we derive an estimate for the norm of the trajectory of a subsystem in a given finite time interval for a linear time invariant system with time varying inputs. In section 4.4 we show that under mild regularity conditions for sufficiently small values of $\|A_o\|$ a fixed point exists. In section 4.5 we derive an estimate for the error $\|x^* - X\|$, and in section 4.6 we provide an estimate for convergence rate of $\mathcal{I}$ and a discussion of the various factors that affect the convergence. Finally, in section 4.7 we study the behavior of DIRM for arbitrarily small time intervals.

4.2. Summary of the results of the analysis. Here we shall provide a summary of the results of the analysis from the rest of the subsections. The reader who is not interested in mathematical details and proofs may read this subsection and then skip to section 5 for numerical examples.

Result 1. For systems that are sufficiently diagonally dominant ($\|A_o\|$ small enough), under further mild regularity conditions a fixed point x^* of $\mathcal{I}$ exists. We do not provide a quantitative bound on $\|A_o\|$. This result is proven in section 4.4. See Proposition 4.5. This result holds for an arbitrary (finite) number of subsystems with possibly different dimensions.

Result 2. Assuming that a fixed point x^* of $\mathcal{I}$ exists we obtain an upper bound (4.21) for the error between the fixed point trajectory x^* and the true solution trajectory X of the system. This is shown in section 4.5. See Proposition 4.8.

Result 3. Assuming that a fixed point x^* of $\mathcal{I}$ exists we obtain an upper bound for $\|D\mathcal{I}(x^*)\|$ (the norm of the linearization of the iteration operator at the fixed point). If $\|D\mathcal{I}(x^*)\| < 1$, then DIRM will converge for all initial iterates $x^{(0)}$ that are sufficiently close to x^*. See section 4.6 and Proposition 4.9.

Result 4. We show that in the case of systems for which a fixed point x^* of DIRM exists for all small enough T, that DIRM converges to x^* for all sufficiently small T if our initial iterate $x^{(0)}$ is sufficiently close to x^*. See section 4.7 and Proposition 4.11.

Remark 4.1. The proof of Results 2 and 3 (and hence that of 4) use the equation (4.4) which holds for two subsystems. We expect "qualitatively" similar results to hold for arbitrary number of subsystems but cannot make any rigorous claims without further analysis. We have limited the analysis to two subsystems because an equation equivalent to (4.4) is combinatorially very cumbersome for the case of more than two subsystems.

The above results do not constitute a comprehensive convergence analysis. For instance we cannot make conclusions about global convergence of DIRM. But these results suggest that DIRM is likely to perform well if certain desirable conditions are met. This has been verified by numerical experiments.

4.3. Finite horizon response of a subsystem. In our analysis of errors and convergence rate we need to estimate the 2-norm of the trajectory of a subsystem in a given finite time interval in response to a forcing term (input) and nontrivial initial conditions for a linear time invariant system. In this section we introduce some relevant notation as well as estimates that will be employed in our later analysis.

Consider the system

$$\dot{x} = Ax + u$$

with input $u(t)$ and initial condition $x(0) = x_0$ in the interval $[0, T]$. We are only interested in $u \in \mathcal{L}_2([0,T], \mathbb{R}^n)$. The solution is

$$x(t) = \int_0^t e^{A(t-\tau)} u(\tau) d\tau + e^{At} x_0.$$

This may be written in the form

$$x = F(T; A)u + G(T; A)x_0, \tag{4.8}$$

where $F(T;A) : \mathcal{L}_2([0,T], \mathbb{R}^n) \to \mathcal{L}_2([0,T], \mathbb{R}^n)$ and $G(T;A) : \mathbb{R}^n \to \mathcal{L}_2([0,T], \mathbb{R}^n)$ are linear operators. It is in general very difficult to obtain sharp estimates for the

norms of $F(T;A)$ and $G(T;A)$, and in fact this basically reduces to the problem of estimating the norm of the matrix exponential. As such we shall not provide an estimate, but we will remark that these norms grow exponentially with T at a rate that is determined by the largest real part of any eigenvalue of A and in addition depend on the nonnormality of A. See [4] for an estimate of the matrix exponential. In our analysis we estimate $\|x\|$ as

$$\|x\| \le \|F(T;A)\|\|u\| + \|G(T;A)\|\|x_0\|, \tag{4.9}$$

expressing the results in terms of $\|F(T;A)\|$ and $\|G(T;A)\|$.

Remark 4.2. Note that the norms on $F(T;A)$ and $G(T;A)$ are the appropriate induced 2-norms.

We shall state and prove a simple lemma on $F(T;A)$ which will be used later.

LEMMA 4.3. $\lim_{T\to 0}\|F(T;A)\| = 0$.

Proof.

$$\begin{aligned}\|F(T;A)u\|^2 &= \int_0^T \left\| \int_0^t e^{A(t-\tau)}u(\tau)d\tau \right\|^2 dt \\ &\le \int_0^T \int_0^t \|e^{A(t-\tau)}\|^2\|u(\tau)\|^2 d\tau dt \\ &\le e^{2\|A\|T}\int_0^T \int_0^T \|u(\tau)\|^2 d\tau dt \\ &= Te^{2\|A\|T}\|u\|^2.\end{aligned}$$

So in fact, as $T \to 0$, $\|F(T;A)\| = \mathrm{O}(\sqrt{T})$. ∎

Now we will focus on a system that consists of two subsystems and obtain an estimate for one of the subsystems that relates the results with the norms of the coupling terms (the off-diagonal blocks) as well as the subsystem properties (diagonal blocks). Consider the coupled systems

$$\begin{aligned}\dot{x}_1 &= A_1x_1 + \kappa A_{12}x_2 + u_1, \\ \dot{x}_2 &= \kappa A_{21}x_1 + A_2x_2 + u_2, \\ x_1(0) = x_{10},\ x_2(0) &= x_{20}\end{aligned} \tag{4.10}$$

in the interval $[0,T]$. Here κ is a "coupling parameter" introduced to aid our analysis. The final results are all evaluated at $\kappa = 1$. We will obtain an estimate for $\|x_1\|$. Since $x_i(t)$ (for $i = 1,2$) is a (vector-valued) entire function of κ we may write it as

$$x_i(t;\kappa) = \sum_{\alpha=0}^{\infty} \kappa^\alpha \frac{\partial^\alpha x_i(t;0)}{\alpha!}, \qquad i = 1,2,$$

where $\partial = \frac{\partial}{\partial\kappa}$, and the series converges for all t and all κ. For $\alpha \ge 1$, $\partial^\alpha x_i(t;0)$ are given by the decoupled equations

$$\begin{aligned}\partial^\alpha \dot{x}_1(t;0) &= A_1\partial^\alpha x_1(t;0) + \alpha A_{12}\partial^{\alpha-1}x_2(t;0), \\ \partial^\alpha \dot{x}_2(t;0) &= A_2\partial^\alpha x_2(t;0) + \alpha A_{21}\partial^{\alpha-1}x_1(t;0), \\ \partial^\alpha x_1(0;0) = 0, &\qquad \partial^\alpha x_2(0;0) = 0.\end{aligned}$$

For the $\alpha = 0$ case we have

$$\begin{aligned}\dot{x}_1(t;0) &= A_1 x_1(t;0) + u_1(t),\\ \dot{x}_2(t;0) &= A_2 x_2(t;0) + u_2(t),\\ x_1(0;0) &= x_{10}, \qquad x_2(0;0) = x_{20}.\end{aligned}$$

Let $x_1(.\,;\kappa)$ denote the function, i.e., $x_1(.\,;\kappa) \in \mathcal{L}_2([0,T],\mathbb{R}^n)$. Setting $\kappa = 1$, from the above equations we can write $x_1(.\,;1)$ as

$$x_1(.\,;1) = \sum_{\alpha=0}^{\infty} F^\alpha x_1(.\,;0) + \sum_{\alpha=0}^{\infty} F^\alpha F_1 A_{12} x_2(.\,;0),$$

where the operators $F_1, F_2, F : \mathcal{L}_2([0,T],\mathbb{R}^n) \to \mathcal{L}_2([0,T],\mathbb{R}^n)$ are defined by $F_i = F(T;A_i)$, for $i = 1,2$, and

$$F = F_1 A_{12} F_2 A_{21}.$$

Assuming $\|F\| < 1$ (which is true for sufficiently small T by Lemma 4.3) we obtain an upper bound for $\|x_1\|$:

$$\|x_1\| \le \sum_{\alpha=0}^{\infty} \|F\|^\alpha \|x_{d1}\| + \sum_{\alpha=0}^{\infty} \|F\|^\alpha \|F_1\| \|A_{12}\| \|x_{d2}\|,$$

where we have dropped the parameter κ altogether and x_{di} for $i = 1,2$ denote the solutions of the decoupled systems: $\dot{x}_{di} = A_i x_{di} + u_i,\ x_{di}(0) = x_{i0}$. Finally, after simplifying the above bound, we obtain the result that, for sufficiently small T,

$$\|x_1\| \le \frac{(\|F_1\|\|u_1\| + \|G_1\|\|x_{10}\|)}{1 - \|F\|} + \frac{\|F_1\|\|A_{12}\|(\|F_2\|\|u_2\| + \|G_2\|\|x_{20}\|)}{1 - \|F\|}, \tag{4.11}$$

where we have used the estimates (4.9) for $\|x_{d1}\|$ and $\|x_{d2}\|$, and $G_i = G(T;A_i)$ for $i = 1,2$.

It is clear that the effect of subsystem 2 on subsystem 1 diminishes as the norm of A_{12} diminishes.

Remark 4.4. It is interesting to note that the κ series expansion mentioned here is intimately related to the Jacobi WR method. In fact the sequence of partial sums of the series for $\kappa = 1$ is the same as the sequence of iterates obtained by applying the Jacobi WR, i.e., WR with the splitting $A = A_d + A_o$, where A_d and A_o are defined by (4.6) and (4.7), respectively, starting with isolated subsystem (couplings assumed zero) solutions as the initial iterate.

4.4. Existence of fixed points of DIRM. In general it is hard to prove the existence of fixed points of the operator $\mathcal{I}$. However, under mild regularity conditions we can show that a fixed point exists for sufficiently small $\|A_o\|$. For this purpose we shall consider the iteration operator $\mathcal{J} : \mathcal{P}^2 \to \mathcal{P}^2$ that maps $P^{(\alpha)}$ to $P^{(\alpha+1)}$. Recalling that $\mathcal{I} = \mathcal{S} \circ \mathcal{R}$ from section 4.1 we see that $\mathcal{J} = \mathcal{R} \circ \mathcal{S}$. It is easy to see that x^* is a fixed point of $\mathcal{I}$ if and only if $P^* = \mathcal{R}x^*$ is a fixed point of $\mathcal{J}$ (provided $\mathcal{R}x^*$ is well defined) and similarly P^* is a fixed point of $\mathcal{J}$ if and only if $x^* = \mathcal{S}P^*$ is a fixed point of $\mathcal{I}$.

PROPOSITION 4.5. *Consider a system with a given diagonal part A_d as defined by* (4.6). *Let $x_d = (x_{d1}, x_{d2})$ be the solution of the decoupled systems; $\dot{x}_d = A_d x_d$, $x_d(0) = x_0$. Let $\nu_1^i \ge \nu_2^i \ge \cdots \ge \nu_n^i \ge 0$ be the eigenvalues of the correlation matrices*

of x_{di} for $i = 1, 2$, respectively. If $\nu_k^i > \nu_{k+1}^i$, for both $i = 1, 2$, then the operator $\mathcal{J}$ (and hence $\mathcal{I}$) has a fixed point for all off-diagonal parts A_o (as defined by (4.7)) in an open neighborhood of the origin in $\mathcal{O} \subset \mathbb{R}^{2n \times 2n}$. Here $\mathcal{O}$ is the $2n^2$ dimensional subspace of all possible off-diagonal parts.

Proof. Write the system $\dot{x} = Ax$ as

$$\dot{x} = A_d x + A_o x,$$

where A_d and A_o are defined according to (4.6) and (4.7), respectively. (Note that $A = A_d + A_o$.) We shall treat A_d as fixed and consider A_o as variable.

A fixed point

$$P^* = \begin{bmatrix} P_1^* & 0_{n\times n} \\ 0_{n\times n} & P_2^* \end{bmatrix}$$

of $\mathcal{J}$ must be such that $P_1 = P_1^*$ is a minimizer of $e_1(P_1, x_1)$ while holding x_1 fixed, and $P_2 = P_2^*$ is a minimizer of $e_2(P_2, x_2)$ while holding x_2 fixed, where $e_i(P_i, x_i)$ are defined by

$$e_i(P_i, x_i) = \int_0^T (P_i x_i(t) - x_i(t))^T (P_i x_i(t) - x_i(t)) dt, \qquad i = 1, 2.$$

Hence by applying the first order optimality conditions we see that $P = P^*$ must be a root of the following system of equations:

$$\begin{aligned} &\frac{\partial e_1}{\partial P_1}(P_1, S_1(P_2; A_o)) = 0, \\ &\frac{\partial e_2}{\partial P_2}(P_2, S_2(P_1; A_o)) = 0, \end{aligned} \tag{4.12}$$

where we have used the fact that $x_1 = x_1^*$ at the fixed point depends on P_2^* and similarly $x_2 = x_2^*$ depends on P_1^*. Here the "solution operator" S_1 maps $P_2^{(\alpha)}$ to $x_1^{(\alpha+1)}$ according to the equations (4.2). The operator S_2 is defined similarly. Note that the operators S_1 and S_2 in general both depend on A_o.

Because of the coupling, it is hard to decide if the system (4.12) has a root in general. However, when $A_o = 0 \in \mathcal{O}$, the original system of ODEs are decoupled and as such S_1 and S_2 are independent of P_2 and P_1, respectively. Hence the equations in (4.12) are decoupled. Furthermore, our assumption that $\nu_k^i > \nu_{k+1}^i$ for both $i = 1, 2$ implies that the two errors e_1 and e_2 can be minimized uniquely and independently according to the POD procedure. This proves the existence of a unique fixed point $P = P^*(A_o = 0)$ of the operator $\mathcal{J}$ for $A_o = 0$. The second order optimality conditions for unique minima imply that both $\frac{\partial^2 e_1}{\partial P_1^2}$ and $\frac{\partial^2 e_2}{\partial P_2^2}$ when evaluated at $A_o = 0$ and $P = P^*(A_o = 0)$ have full rank.

Therefore it also follows that the Jacobian

$$\begin{bmatrix} \frac{\partial^2 e_1}{\partial P_1^2} & \frac{\partial^2 e_1}{\partial P_1 \partial P_2} \\ \frac{\partial^2 e_2}{\partial P_1 \partial P_2} & \frac{\partial^2 e_2}{\partial P_2^2} \end{bmatrix}$$

is full rank for $A_o = 0$ and $P = P^*(A_o = 0)$. Hence, by the implicit function theorem, we conclude that a root $P = P^*(A_o)$ of (4.12) exists for all A_o in an open neighborhood of $0 \in \mathcal{O}$. Furthermore, by continuity it follows that $\frac{\partial^2 e_1}{\partial P_1^2}$ and $\frac{\partial^2 e_2}{\partial P_2^2}$ have

full rank for $(A_o, P = P^*(A_o))$ for all A_o in some open neighborhood of $0 \in \mathcal{O}$. This establishes $P = P^*(A_o)$ as a fixed point of $\mathcal{J}$ for all A_o in an open neighborhood of $0 \in \mathcal{O}$. ∎

COROLLARY 4.6. *Under similar assumptions Proposition* 4.5 *holds for an arbitrary number m of subsystems of possibly different dimensions.*

Proof. Follow the same line of reasoning with (4.12) replaced by

$$\frac{\partial e_i}{\partial P_i}(P_i, S_i(P_1, \ldots, P_{i-1}, P_{i+1}, \ldots, P_m; A_o)) = 0, \qquad i = 1, \ldots, m. \tag{4.13}$$

The key point is that the operator S_i does not depend on P_i. ∎

Remark 4.7. Ideally we would like to show that for any value of $\|A_o\|$ a fixed point exists for sufficiently small T. The intuition is that when T gets arbitrarily small, the trajectories are increasingly well approximated by straight lines. However, we do not have a proof yet.

4.5. Accuracy of DIRM. We will introduce a few new variables to facilitate our analysis. Given $P^{(\alpha)}, x^{(\alpha)}, \hat{x}^{(\alpha)}$, and X as defined in section 4.1, define $v^{(\alpha)}, w^{(\alpha)}$, and $\xi^{(\alpha)}$ as follows:

$$v^{(\alpha)} = P^{(\alpha-1)}x^{(\alpha)} - x^{(\alpha)}, \tag{4.14}$$

$$w^{(\alpha)} = \hat{x}^{(\alpha)} - P^{(\alpha-1)}x^{(\alpha)}, \tag{4.15}$$

and

$$\xi^{(\alpha)} = x^{(\alpha)} - X. \tag{4.16}$$

We may think of $v^{(\alpha)}$ as a "difference" trajectory that measures the gap between $x^{(\alpha)}$ and its projection $P^{(\alpha-1)}x^{(\alpha)}$ and $w^{(\alpha)}$ as a difference trajectory that measures the gap between the reduced trajectory $\hat{x}^{(\alpha)}$ and $P^{(\alpha-1)}x^{(\alpha)}$. The trajectory $\xi^{(\alpha)}$ is the error between the true solution and the DIRM iterate at step α.

Suppose x^* is a fixed point of $\mathcal{I}$. Assume $P^* = \mathcal{R}x^*$ is well defined. Let $\hat{x}^*, v^*, w^*$, and ξ^* be the corresponding fixed point trajectories. Note that the error in using DIRM is ξ^*. We will provide an estimate of $\|\xi^*\|$. Substituting $v^{(\alpha)} = v^*$, $P^{(\alpha-1)} = P^*$, and $x^{(\alpha)} = x^*$ in (4.14), we obtain

$$v^* = P^*x^* - x^*.$$

Similarly we obtain $w^* = \hat{x}^* - P^*x^*$ from (4.15). Note that these two relations imply that $\hat{x}^* - x^* = v^* + w^*$. Differentiating $w^* = \hat{x}^* - P^*x^*$ with respect to time, and using (4.4), we obtain

$$\begin{aligned} \dot{w}^* &= P^*A_d\hat{x}^* + P^*A_ox^* - P^*A_dx^* - P^*A_o\hat{x}^* \\ &= P^*(A_d - A_o)(\hat{x}^* - x^*). \end{aligned}$$

Hence we obtain the following differential equation for w^*:

$$\dot{w}^* = P^*(A_d - A_o)w^* + P^*(A_d - A_o)v^*, \qquad w^*(0) = 0. \tag{4.17}$$

Similarly (4.16) implies $\xi^* = x^* - X$. Differentiating and using (4.4), and $\dot{X} = AX = (A_d + A_o)X$, we obtain

$$\begin{aligned}\dot{\xi}^* &= A_d x^* + A_o \hat{x}^* - AX \\ &= A(x^* - X) + A_o(\hat{x}^* - x^*).\end{aligned}$$

Using $\hat{x}^* - x^* = v^* + w^*$ we write the equation for ξ^* as

$$\dot{\xi}^* = A\xi^* + A_o(v^* + w^*), \qquad \xi^*(0) = 0. \tag{4.18}$$

From the application of the estimate (4.9) to (4.17) we obtain that

$$\|w^*\| \leq \|F(T; P^*(A_d - A_o))\|\|A_d - A_o\|\|v^*\|. \tag{4.19}$$

Applying the estimate (4.9) to (4.18) and using the above equation we obtain

$$\|\xi^*\| \leq \|F(T; A)\|\|A_o\| \left\{1 + F(T; P^*(A_d - A_o))\|A_d - A_o\|\right\} \|v^*\|. \tag{4.20}$$

The quantity $\|v^*\|$ is the sum of the POD projection errors $\|P_i^* x_i - x_i\|$ of both the subsystems. This quantity is the same as the square root of the sum of the eigenvalues of the neglected modes summed over both the subsystems. Note that if the POD projection error of the fixed point trajectory is zero, then the error of the converged DIRM solution is zero. It is also clear that the error depends on the norm of the off-diagonal blocks A_o, on the norm of the exponentials of A and $P^*(A_d - A_o)$, as well as on the time interval T.

We have thus proved the following proposition.

PROPOSITION 4.8. *Let x^* be a fixed point of $\mathcal{I}$ and suppose that $P^* = \mathcal{R}x^*$ is well defined. Let X be the true solution: $\dot{X} = AX$; $X(0) = x_0$. Then the error $\|x^* - X\|$ (2-norm) satisfies*

$$\|x^* - X\| \leq \|F(T; A)\|\|A_o\| \left\{1 + F(T; P^*(A_d - A_o))\|A_d - A_o\|\right\} \|v^*\|, \tag{4.21}$$

where $\|v^*\| = \|P^* x^* - x^*\|$ is the projection error of the fixed point trajectory.

4.6. Rate of convergence. In this section, we will compute an upper bound for $\|D\mathcal{I}(x^*)\|$, the norm of the linearization of the iteration $\mathcal{I}$ at a fixed point x^*. First, we will compute $\delta x^{(\alpha+1)} = D\mathcal{I}(x^{(\alpha)})(\delta x^{(\alpha)})$, which is the variation in $x^{(\alpha+1)}$ due to a variation $\delta x^{(\alpha)}$ in $x^{(\alpha)}$. The notation $D\mathcal{I}(x)(\delta x)$ denotes the directional derivative of the operator $\mathcal{I}$ evaluated at $x \in \mathcal{L}_2([0,T], \mathbb{R}^{2n})$ in the direction $\delta x \in \mathcal{L}_2([0,T], \mathbb{R}^{2n})$. The variations of all quantities will be denoted by the prefix δ, except that the variation of $P^{(\alpha)}$ will be denoted by $E^{(\alpha)}$. In our analysis the norm used for the variations of trajectories will also be the 2-norm, and the norms of matrices will be the induced 2-norm.

Again we shall make use of the difference trajectories $v^{(\alpha)}$ and $w^{(\alpha)}$ as defined by (4.14) and (4.15). Taking variations of (4.14) (with α replaced by $\alpha + 1$) it follows that

$$\delta v^{(\alpha+1)} = E^{(\alpha)} x^{(\alpha+1)} + \left(P^{(\alpha)} - 1\right) \delta x^{(\alpha+1)}. \tag{4.22}$$

Following a procedure similar to the one that was used to obtain (4.18), we obtain from (4.16) the following equation for $\xi^{(\alpha+1)}$:

$$\dot{\xi}^{(\alpha+1)} = A\xi^{(\alpha+1)} + A_o\left(v^{(\alpha+1)} + w^{(\alpha+1)}\right), \qquad \xi^{(\alpha+1)}(0) = 0.$$

From (4.16) we also see that $\delta x^{(\alpha)} = \delta\xi^{(\alpha)}$. Therefore, taking variations of the above equation, we get

$$\delta\dot{x}^{(\alpha+1)} = A\delta x^{(\alpha+1)} + A_o\delta v^{(\alpha+1)} + A_o\delta w^{(\alpha+1)}, \qquad \delta x^{(\alpha+1)}(0) = 0. \tag{4.23}$$

Following a procedure similar to the one that was used to obtain (4.17), we obtain from (4.15) the following equation for $w^{(\alpha+1)}$:

$$\begin{aligned} \dot{w}^{(\alpha+1)} &= P^{(\alpha)}(A_d - A_o)w^{(\alpha+1)} + P^{(\alpha)}(A_d - A_o)v^{(\alpha+1)}, \\ w^{(\alpha+1)}(0) &= 0. \end{aligned} \tag{4.24}$$

Hence the variation $\delta w^{(\alpha+1)}$ is given by

$$\begin{aligned} \delta\dot{w}^{(\alpha+1)} &= P^{(\alpha)}(A_d - A_o)\delta w^{(\alpha+1)} + P^{(\alpha)}(A_d - A_o)\delta v^{(\alpha+1)} \\ &\quad + E^{(\alpha)}(A_d - A_o)\left(w^{(\alpha+1)} + v^{(\alpha+1)}\right), \quad \delta w^{(\alpha+1)}(0) = 0. \end{aligned} \tag{4.25}$$

Substituting for $\delta v^{(\alpha+1)}$ from (4.22) into (4.23) and (4.25) we get a coupled system of equations for $\delta x^{(\alpha+1)}$ and $\delta w^{(\alpha+1)}$:

$$\begin{aligned} \delta\dot{x}^{(\alpha+1)} &= (A + A_o(P^{(\alpha)} - 1))\delta x^{(\alpha+1)} + A_o\delta w^{(\alpha+1)} + A_oE^{(\alpha)}x^{(\alpha+1)}, \\ \delta\dot{w}^{(\alpha+1)} &= P^{(\alpha)}(A_d - A_o)\left(P^{(\alpha)} - 1\right)\delta x^{(\alpha+1)} + P^{(\alpha)}(A_d - A_o)\delta w^{(\alpha+1)} \\ &\quad + P^{(\alpha)}(A_d - A_o)E^{(\alpha)}x^{(\alpha+1)} + E^{(\alpha)}(A_d - A_o)\left(w^{(\alpha+1)} + v^{(\alpha+1)}\right), \\ \delta x^{(\alpha+1)}(0) &= 0, \qquad \delta w^{(\alpha+1)}(0) = 0. \end{aligned} \tag{4.26}$$

Note that the above system is driven by terms containing $x^{(\alpha+1)}$, $v^{(\alpha+1)}$, and $w^{(\alpha+1)}$. Since we are interested in perturbations about the fixed point x^*, we set

$$\begin{aligned} x^{(\alpha+1)} &= x^{(\alpha)} = x^*, \\ v^{(\alpha+1)} &= v^{(\alpha)} = v^*, \\ w^{(\alpha+1)} &= w^{(\alpha)} = w^*. \end{aligned}$$

Also we shall denote $\delta x^{(\alpha)} = \delta x$ and write $E^{(\alpha)}$ and $\delta x^{(\alpha+1)}$ as

$$\begin{aligned} E^{(\alpha)} &= \frac{dP}{dx}(x^*)(\delta x), \\ \delta x^{(\alpha+1)} &= D\mathcal{I}(x^*)(\delta x). \end{aligned}$$

Note that $\frac{dP}{dx}(x^*)(\delta x)$, which may also be written as $D\mathcal{R}(x^*)(\delta x)$, is the directional derivative of $P = \mathcal{R}(x)$ at $x = x^*$ in the direction δx. For sufficiently small T we apply the estimate (4.11) to (4.26) at a fixed point and obtain

$$\begin{aligned} \|D\mathcal{I}(x^*)(\delta x)\| &\le \frac{\|F_1\|}{(1 - \|F\|)}\left\|A_oP^*\frac{dP}{dx}(x^*)(\delta x)x^*\right\| \\ &+ \frac{\|F_1\|\|F_2\|\|A_o\|}{(1 - \|F\|)}\left\|P^*(A_d - A_o)\frac{dP}{dx}(x^*)(\delta x)x^* + \frac{dP}{dx}(x^*)(\delta x)(A_d - A_o)(w^* + v^*)\right\|, \end{aligned}$$

where

$$\begin{aligned} F_1 &= F(T; A + A_o(P^* - 1)), \\ F_2 &= F(T; P^*(A_d - A_o)), \\ F &= F_1A_oF_2P^*(A_d - A_o)(P^* - 1). \end{aligned} \tag{4.27}$$

We simplify further and write

$$\|D\mathcal{I}(x^*)(\delta x)\| \le \frac{\|F_1\|\|A_o\|}{(1-\|F\|)}H,$$

where the term H is given by

$$H = \left\|\frac{dP}{dx}(x^*)(\delta x)x^*\right\| + \|F_2\|\|A_d - A_o\|\left(\left\|\frac{dP}{dx}(x^*)(\delta x)x^*\right\| + \left\|\frac{dP}{dx}(x^*)(\delta x)\right\|\|v^* + w^*\|\right).$$

Using the estimate (4.19) one can obtain an upper bound for H which does not contain w^*. After rearranging some terms we obtain the upper bound

$$\|D\mathcal{I}(x^*)(\delta x)\| \le \frac{\|F_1\|\|A_o\|(1+\|F_2\|\|A_d - A_o\|)}{(1-\|F\|)} \times \left(\left\|\frac{dP}{dx}(x^*)(\delta x)x^*\right\| + \left\|\frac{dP}{dx}(x^*)(\delta x)\right\|\|F_2\|\|A_d - A_o\|\|v^*\|\right).$$

Taking the supremum over all unit norm variations δx, we obtain the bound

$$\|D\mathcal{I}(x^*)\| \le \frac{\|F_1\|\|A_o\|(1+\|F_2\|\|A_d - A_o\|)}{(1-\|F\|)} \times \left(\sup_{\|\delta x\|=1}\left\{\left\|\frac{dP}{dx}(x^*)(\delta x)x^*\right\|\right\} + \left\|\frac{dP}{dx}(x^*)\right\|\|F_2\|\|A_d - A_o\|\|v^*\|\right).$$

The sensitivity of the POD projection matrix $P(x)$ to perturbations in the trajectory x has been studied and quantified in [13]. It follows directly from the results in [13] that

$$\left\|\frac{dP}{dx}(x^*)\right\|_{\mathrm{F}} = \max_{i\le k,\, j\le n-k}\sqrt{2}\frac{\sqrt{\lambda_i^1+\lambda_{j+k}^1}}{\lambda_i^1-\lambda_{j+k}^1} + \max_{i\le k,\, j\le n-k}\sqrt{2}\frac{\sqrt{\lambda_i^2+\lambda_{j+k}^2}}{\lambda_i^2-\lambda_{j+k}^2}, \tag{4.28}$$

$$\sup_{\|\delta x\|=1}\left\{\left\|\frac{dP}{dx}(x^*)(\delta x)x^*\right\|\right\} = \left(\frac{\lambda_k^1+\lambda_{k+1}^1}{\lambda_k^1-\lambda_{k+1}^1}\right) + \left(\frac{\lambda_k^2+\lambda_{k+1}^2}{\lambda_k^2-\lambda_{k+1}^2}\right),$$

where $\lambda_1^i \ge \lambda_2^i \ge \cdots \ge \lambda_n^i$ are the ordered eigenvalues of the correlation matrix of the fixed point trajectories x_i^*, for $i = 1, 2$, and the subscript "F" denotes the Frobenius norm. Note that we have assumed that $\lambda_k^i > \lambda_{k+1}^i$, for $i = 1, 2$, in order for P^* to be well defined. Also note that $\|v^*\|$ is given by

$$\|v^*\| = \sqrt{\lambda_{k+1}^1 + \cdots + \lambda_n^1 + \lambda_{k+1}^2 + \cdots + \lambda_n^2}.$$

Since $\|\frac{dP}{dx}(x^*)\|_2 \le \|\frac{dP}{dx}(x^*)\|_{\mathrm{F}}$, using the expression for $\|v^*\|$ we may obtain an upper bound for $\|D\mathcal{I}(x^*)\|$ which we shall state as a proposition.

PROPOSITION 4.9. *Suppose $x^* = (x_1^*, x_2^*)$ is a fixed point of $\mathcal{I}$ and assume that $P^* = \mathcal{R}x^*$ is well defined. Then, for sufficiently small T, $\|D\mathcal{I}(x^*)\|$ satisfies*

$$\|D\mathcal{I}(x^*)\| \le \frac{\|F_1\|\|A_o\|}{(1-\|F\|)}(1+\|F_2\|\|A_d - A_o\|)\{\mathcal{C}_1(\lambda) + \mathcal{C}_2(\lambda)\|F_2\|\|A_d - A_o\|\}, \tag{4.29}$$

where $\mathcal{C}_1$ and $\mathcal{C}_2$ are functions of the eigenvalues λ of the correlation matrices of the fixed point trajectories x_1^* and x_2^* given by

$$\begin{aligned}
\mathcal{C}_1 &= \left(\frac{\lambda_k^1+\lambda_{k+1}^1}{\lambda_k^1-\lambda_{k+1}^1}\right)+\left(\frac{\lambda_k^2+\lambda_{k+1}^2}{\lambda_k^2-\lambda_{k+1}^2}\right),\\
\mathcal{C}_2 &= \left(\max_{i\le k,\, j\le n-k}\sqrt{2}\frac{\sqrt{\lambda_i^1+\lambda_{j+k}^1}}{\lambda_i^1-\lambda_{j+k}^1}+\max_{i\le k,\, j\le n-k}\sqrt{2}\frac{\sqrt{\lambda_i^2+\lambda_{j+k}^2}}{\lambda_i^2-\lambda_{j+k}^2}\right)\\
&\quad\times\sqrt{\lambda_{k+1}^1+\cdots+\lambda_n^1+\lambda_{k+1}^2+\cdots+\lambda_n^2},
\end{aligned}\tag{4.30}$$

and F_1, F_2, and F are as defined in (4.27).

It can be seen from the above results that the convergence rate becomes arbitrarily fast as $\|A_o\|$ becomes arbitrarily small, which agrees with intuition. We also see that the convergence is faster when the POD error is small. However, when the POD error is zero ($\lambda_{k+1}^1+\cdots+\lambda_n^1+\lambda_{k+1}^2+\cdots+\lambda_n^2=0$), the above expression does not predict arbitrarily fast convergence. This may seem counterintuitive. However, one needs to consider this more carefully. The quantity $\|v^*\|=\lambda_{k+1}^1+\cdots+\lambda_n^1+\lambda_{k+1}^2+\cdots+\lambda_n^2$ is the POD projection error of the fixed point trajectory. Even if this is zero, $\|v\|$ corresponding to a nearby trajectory x need not be. Convergence depends on the behavior of nearby trajectories as well. This is evident from the numerical example in section 5.4. If, however, all subsystem trajectories always lie in some k dimensional subspace, then it is clear that DIRM will converge after one iteration. In terms of the above analysis this corresponds to $P^{(\alpha)}$ being constant and $v^{(\alpha+1)}=0$ for all α. Hence $E^{(\alpha)}=0$ and $\delta v^{(\alpha+1)}=0$. Then from (4.24) we see that $w^{(\alpha+1)}=0$ as well. All these together and (4.26) imply that $\delta x^{(\alpha+1)}=0$, indicating immediate convergence.

The analysis also suggests that when the eigenvalues λ_k^1 and λ_{k+1}^1 (or λ_k^2 and λ_{k+1}^2) are very close to each other we may expect difficulties in convergence, since both $\mathcal{C}_1$ and $\mathcal{C}_2$ become very large. This is numerically evident from the example of section 5.3.

4.7. Small time interval case. In this section we consider the convergence behavior of DIRM as $T\to 0$. First let us state and prove the following lemma.

LEMMA 4.10. *Let $z:[0,T_0]\to\mathbb{R}^n$ be a C^n-smooth trajectory. Let $0<T<T_0$ and let $\lambda_1\ge\lambda_2\cdots\ge\lambda_n\ge 0$ be the eigenvalues of the correlation matrix of $z:[0,T]\to\mathbb{R}^n$. Hence λ_i are functions of T. Furthermore, suppose the values of z and its first $n-1$ derivatives at $t=0$ form a linearly independent set. Note that this assumption is generically true in the sense that it holds for an open and dense subset (in $\mathbb{R}^{n(n-1)}$) of possible values of $z(t)$ and its first $n-1$ derivatives at $t=0$. Then, as $T\to 0$, $\lambda_{j+1}/\lambda_j\to 0$ for any $1\le j\le n-1$.*

Proof. In order to keep the proof concise, we shall prove for the case when $z(t)$ is analytic. The proof for C^n is similar. By assumption the set

$$\{z(0), z^{(1)}(0),\ldots,z^{(n-1)}(0)\}$$

is linearly independent, where $z^{(j)}(t)$ denotes the jth derivative of $z(t)$. Since the correlation matrix $R=\int_0^T z(t)z^T(t)dt$ is analytic in T, using Taylor expansion we may write it as

$$R=\sum_{j=1}^{\infty} r_j T^j,$$

where after simplification

$$r_j = \frac{1}{j}\sum_{l=1}^{j} \frac{z^{(l-1)}(0)}{(l-1)!}\frac{(z^{(j-l)}(0))^T}{(j-l)!}, \qquad j = 1, 2, \ldots.$$

Note that when $z(t)$ is C^n, R is C^{n+1} smooth in T, and we should use Taylor's theorem with the remainder term which is $O(T^{n+1})$.

It is clear that $\text{Image}(r_j) = \text{span}\{z(0), z^{(1)}(0), \ldots, z^{(j-1)}(0)\}$ and that $\text{Null}(r_j) = \text{Image}(r_j)^{\perp}$. Hence by our assumption it follows that $\text{rank}\,(r_j) = j$ for $j = 1, \ldots, n$. Let $\mu_1^j \geq \mu_2^j \geq \cdots \geq \mu_n^j \geq 0$ be the eigenvalues of r_j for all j. Note that $\mu_j^j > 0$ and $\mu_l^j = 0$ for $l = j+1, \ldots, n$, and $j = 1, \ldots, n$.

Define partial sums

$$R_j = \sum_{l=1}^{j} r_l T^l$$

for $j = 1, \ldots, n$. Let $\nu_1^j \geq \nu_2^j \geq \cdots \geq \nu_n^j \geq 0$ be the eigenvalues of R_j. Since $\text{Image}(r_{j-1}) \subset \text{Image}(r_j)$, for $j = 1, \ldots, n$, it follows that $\text{rank}(R_j) = \text{rank}(r_j) = j$ for $j = 1, \ldots, n$. Hence $\nu_j^j > 0$ and $\nu_l^j = 0$ for $l = j+1, \ldots, n$ and $j = 1, \ldots, n$. Since $R_j = R_{j-1} + T^j r_j$, for $j = 1, \ldots, n$, using Theorem 8.1.5 of [4] on symmetric eigenvalue perturbations, we see that $\nu_j^j \leq \nu_j^{j-1} + T^j \mu_1^j$. The same theorem also yields $\nu_n^{j-1} + T^j \mu_j^j \leq \nu_j^j$. Since $\nu_n^{j-1} = \nu_j^{j-1} = 0$, we get

$$0 < T^j \mu_j^j \leq \nu_j^j \leq T^j \mu_1^j, \qquad j = 1, \ldots, n. \tag{4.31}$$

For $j = 1, \ldots, n$ we may write R as

$$R = R_j + T^{j+1} N_{j+1},$$

where $N_{j+1} = \sum_{l=1}^{\infty} r_{j+l} T^{l-1}$. Let $\tilde{\nu}_1^j \geq \tilde{\nu}_2^j \geq \cdots \geq \tilde{\nu}_n^j \geq 0$ be the eigenvalues of N_j for $j = 2, \ldots, n+1$. Application of Theorem 8.1.5 of [4] to $R = R_j + T^{j+1} N_{j+1}$ yields

$$\nu_j^j + T^{j+1}\tilde{\nu}_n^{j+1} \leq \lambda_j \leq \nu_j^j + T^{j+1}\tilde{\nu}_1^{j+1}, \qquad j = 1, \ldots, n.$$

This together with (4.31) implies

$$0 < T^j \mu_j^j \leq \lambda_j \leq T^j \mu_1^j + T^{j+1}\tilde{\nu}_1^{j+1}, \qquad j = 1, \ldots, n. \tag{4.32}$$

This yields

$$\frac{\lambda_{j+1}}{\lambda_j} \leq T\left(\frac{\mu_1^{j+1}}{\mu_j^j} + T\tilde{\nu}_1^{j+2}\right), \qquad j = 1, \ldots, n-1.$$

Since $\lim_{T\to 0} N_{j+2} = r_{j+2}$, by continuity $\lim_{T\to 0} \tilde{\nu}_1^{j+2} = \mu_1^{j+2}$ which is finite. Hence $\lim_{T\to 0} \frac{\lambda_{j+1}}{\lambda_j} = 0$ for $j = 1, \ldots, n-1$. ∎

Now we state the following proposition about convergence of DIRM in the limit $T \to 0$.

PROPOSITION 4.11. *Suppose there exists a T_1 such that for all $T < T_1$ a fixed point x^* of $\mathcal{I}$ exists and that $P^* = \mathcal{R}x^*$ is well defined. Further suppose x^* satisfies the*

conditions of Lemma 4.10. *Let* X *be the true solution. Then there exists a* $T_0 < T_1$ *such that DIRM converges to* x^**, for all* $T < T_0$*, for initial guesses* $x^{(0)}$ *that are sufficiently close to* x^*.

Proof. Application of Lemma 4.10 immediately yields that

$$\lim_{T\to 0} \mathcal{C}_1 = 2$$

and

$$\lim_{T\to 0} \mathcal{C}_2 = 0.$$

Also, as $T \to 0$, both $\|F_1\|$ and $\|F_2\| \to 0$ (Lemma 4.3), and hence $\|F\| \to 0$ as well. So $\|D\mathcal{I}(x^*)\| \to 0$ as $T \to 0$, and in particular $\|D\mathcal{I}(x^*)\| < 1$ for all small enough T. Hence DIRM will converge for all initial guesses $x^{(0)}$ that are sufficiently close to x^*. ∎

5. Examples.

5.1. Example: Nonlinear power grid. In this section we present a power grid model and apply the DIRM method to simulate the transient behavior. The model has been taken from the paper [11]. The model equations we use represent the coupling between power flows and frequency variations across power networks and are known as the *swing equations*. Swing dynamics potentially interact with protection mechanisms and may lead to cascading failures. See [11] for more details.

We used a power grid consisting of 36 nodes arranged in a 6×6 square grid. Each node is either a generator or a load. For general types of load situations we would need DAEs to represent the system. Here we assume that the loads are all synchronous motors. In that case the swing equations involve the variables δ_i, where indices $i = 1, \ldots, N$ denote the nodes ($N = 36$ in our example). Physically at node i, δ_i stands for the generator or motor rotor angle with respect to a synchronously rotating reference frame. The equations are then given by

$$M_i\ddot{\delta}_i + D_i\dot{\delta}_i = P_{mi} - P_{gi}, \qquad i = 1, \ldots, N, \tag{5.1}$$

where M_i and D_i are inertia and damping terms for the generator or motor at the ith node and P_{mi} is the mechanical power input to the generator or the mechanical power output (negative) of the motor at the ith node, and P_{gi} is the electrical power output from the ith node. It is assumed that the voltage magnitudes at the nodes are maintained fixed by regulators. The electrical power P_{gi} is given by

$$\begin{aligned} P_{gi} = Re(V_i^* I_i) &= Re\left(V_i^* \sum_{j=1}^{N} Y_{ij} V_j\right) \\ &= -\sum_{j=1}^{N} |V_i||V_j| b_{ij} \sin(\delta_i(t) - \delta_j(t)), \qquad i = 1, \ldots, N, \end{aligned} \tag{5.2}$$

where $V_i = |V_i|e^{i\delta_i}$, and $Y = G + iB$ is the admittance matrix for the network connections (with some of the i denoting $\sqrt{-1}$). We assume that the lines are lossless ($G = 0$). The b_{ij} are the terms of the *susceptance* matrix B. The diagonal entrees b_{ii} are all zero. If a line is not present between nodes i and j, then $b_{ij} = 0$. We chose $b_{ij} = 1$ for all connected lines.

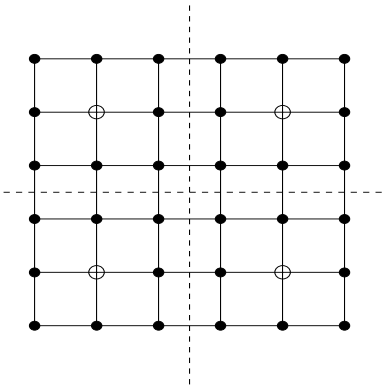

FIG. 5.1. *Power grid: generators—open circles; loads—filled circles.*

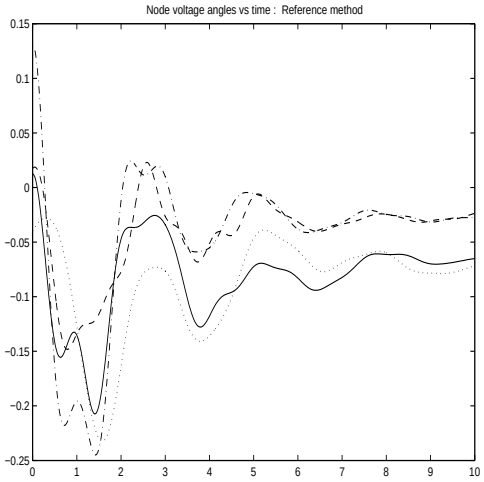

FIG. 5.2. δ_i *vs. time: reference method.*

The grid we chose is shown in Figure 5.1. The generators are marked by open circles, and all other nodes (filled circles) are motors. All physical parameters chosen were nondimensional. We chose all the voltage magnitudes to be the same (constant) value of 1. The mechanical powers P_{mi} were chosen to be -0.0880 for the motor nodes, and generator powers were all 0.7040 so that the total sums to zero. The parameter values $M_i = 2.0$ and $D_i = 0.8$ were chosen for the generators, while values $M_i = 0.1$ and $D_i = 0.1$ were chosen for all load motors. Given these parameters the swing equations have a nontrivial (not all δ_i are zero) steady state solution. We picked a random initial condition (Gaussian with zero mean and 0.1 standard deviation for both δ_i and $\dot{\delta}_i$ for all i). First, we used the MATLAB ODE solver `ode15s` to solve the equations in the interval $[0, 10]$, which indicated that the steady state was more or less reached in that time interval. A plot of the "reference solution" for δ_i for four of the nodes is shown in Figure 5.2. One motor node from each subsystem was chosen for this plot. In order to apply the DIRM method we modularized the system so that the square grid of 6×6 nodes was split into four subsystems, each consisting of a

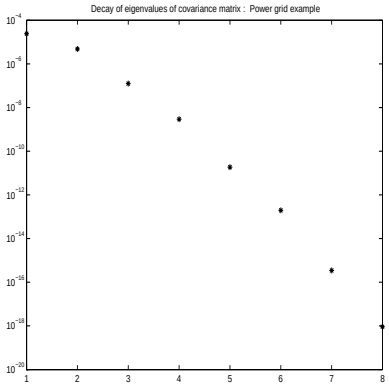

FIG. 5.3. *Decay of POD mode energies: power grid example.*

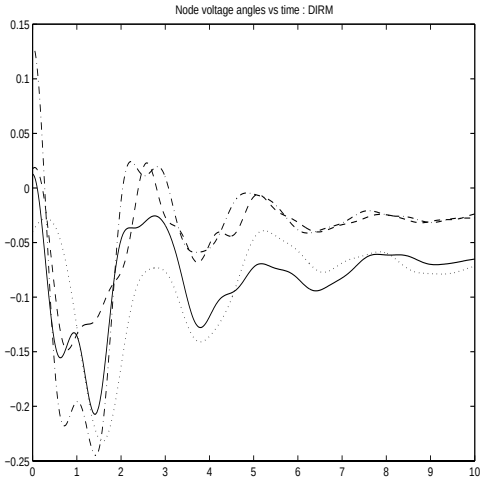

FIG. 5.4. δ_i *vs time: DIRM.*

square subgrid of 3×3 nodes. The broken lines in Figure 5.1 show this partitioning. DIRM did not converge when the simulation interval was $[0, 10]$. However, breaking the interval into smaller intervals achieved convergence. Using intervals of length 0.5 (i.e. $[0, 0.5]$, $[0.51]$, $\ldots$, $[9.5, 10]$) achieved convergence. We used the same MATLAB solver `ode15s` as the underlying solver. Within each interval at most seven iterations were required. The final value of the solution from one interval was used as the initial condition for the next interval. Initial reduced models were obtained by simulating each subsystem in isolation (all other subsystem states were assumed to remain zero) for the time interval under consideration. The reduced order models of all subsystems were chosen to be of dimension 3. (The full dimension of each subsystem is 18.) Figure 5.3 shows the largest eight eigenvalues of the DIRM solution for the first subsystem trajectory in the final simulation interval $[9.5, 10]$. The decay was similar for the other subsystems as well.

The solution obtained using DIRM is shown in Figure 5.4 for the same nodes as in Figure 5.2. The solutions of the reference method and DIRM are visually

indistinguishable and so we plotted them on separate figures. We also computed the maximum relative error e_r defined by

$$e_r = \sup_i \frac{\sup_{t\in[0,10]} |\hat{x}_i(t) - x_i(t)|}{\sup_{t\in[0,10]} |x_i(t)|}, \tag{5.3}$$

where i indexed over all states (node voltage phases and velocities). It was $e_r = 0.0037$; i.e., the relative error for any state variable was less than 0.37%.

An important point during swing dynamic transients is that large deviations of δ_i and $\dot{\delta}_i$ can trigger protection mechanisms that can shut down a line or a generator, and this changes the system parameters discontinuously (some b_{ij} change to 0, for instance) which in turn leads to further transients and so on (see [11]). Since our scheme predicts the solutions accurately, we expect it to predict the first failure (location and time) accurately. However, for accurate prediction beyond the first failure, we have to restart our iteration for a time interval beginning at the failure. Numerical simulations done by Cao and Petzold [1] revealed that the reduced model formed from trajectories obtained before a failure was not accurate after the failure and could not be used to predict further failures. If we include failures in our model, our iterative method may need to be modified. During the iterative simulations, if a subsystem indicates failure, then the time interval of simulation may be shortened so that the reduced models remain more accurate. We have not yet numerically investigated this type of scenario. This is a subject of future research.

5.2. PDE Example: Comparison with WR. We considered the reaction-convection-diffusion equation

$$x_t = \nu x_{ss} + a x_s + b x \tag{5.4}$$

in one spatial variable s in the interval $s \in [0, 6]$ with spatial discretization giving 100 equally spaced interior points. Both first and second spatial derivatives were approximated by centered differences. We used the triangular function

$$\begin{aligned} &x(0,s) = s/3, \qquad 0 \le s \le 3, \\ &x(0,s) = 1 - (s-3)/3, \qquad 3 \le s \le 6, \end{aligned} \tag{5.5}$$

as initial condition, and the boundary conditions were zero. This results in a tridiagonal linear system (ODE) of the form

$$\dot{x} = Ax,$$

where $x \in \mathbb{R}^{100}$.

For DIRM we divided the system into 10 subsystems each of size 10 consisting of adjacent grid points. For WR we used the splitting $A = A_d + A_o$, where A_d is block diagonal with 10×10 blocks and A_o the remaining off-diagonal coupling part. This corresponds to the Jacobi version of WR. We also used overlapping for WR in order to improve its convergence. It is known from the work of Miekkala that in the case of tridiagonal systems the order of convergence of WR is $\omega = 1$ (as defined by [8]), which is very slow. However, if we overlap by o variables, then $\omega = \frac{1}{o+1}$, and this should improve the asymptotic convergence [8].

Simulations of three different sets of parameter values are discussed here. In all cases we computed the solutions using the MATLAB ODE solver `ode15s` to provide a benchmark. The same solver was also used within DIRM and WR. In all simulations of DIRM and WR we used the convergence tolerance (see (3.3)) $tol = 0.001$ and a

TABLE 5.1
Convergence and accuracy of DIRM and WR for the 1D PDE with convection and diffusion. Parameter values $\nu = 0.1, a = 1, b = 0$. Simulation interval $[0, 10]$. Subsystem reduced model dimension $k = 3$.

	Number of iterations	Maximum error over subsystems
DIRM	3	1.3112×10^{-3}
WR overlap $o = 3$	21	12.2107×10^{-3}
WR (no overlap)	> 30 (did not converge)	241.8189×10^{-3}

TABLE 5.2
Convergence and accuracy of DIRM and WR for the 1D PDE with reaction, convection, and diffusion. Parameter values $\nu = 0.1, a = 6, b = 6$. Simulation interval $[0, 1.2]$. Subsystem reduced model dimension $k = 3$.

	Number of iterations	Maximum error over subsystems
DIRM	11	0.5284
WR overlap $o = 3$	16	0.7861
WR (no overlap)	> 30	39.5314

TABLE 5.3
Convergence and accuracy of DIRM and WR for the 1D PDE with pure diffusion. Parameter values $\nu = 0.1, a = 0, b = 0$. Simulation interval $[0, 10]$. Subsystem reduced model dimension $k = 3$.

	Number of iterations	Maximum error over subsystems
DIRM	2	0.4511×10^{-3}
WR overlap $o = 5$	21	1.9688×10^{-3}

maximum iteration count of 30. All the subsystem reduced models in DIRM were of dimension $k = 3$. The convergence and error results are summarized in Tables 5.1, 5.2, and 5.3. The error is measured by $\sup\{\|\hat{x}_i(t) - x_i(t)\|_2 : t \in [0, T],\ i = 1, \ldots, 10\}$, where $x_i(t)$ and $\hat{x}_i(t)$ are the benchmark solution and the iterative method (DIRM or WR) solution of the ith subsystem, respectively. The WR method in general needed some overlapping to achieve convergence. Especially the pure diffusion case required a greater overlap without which WR did not converge at all.

Note that couplings exist only between adjacent subsystems. This is essentially a property of 1D PDEs. Thus for the WR method we expect at least 10 iterations before the first subsystem "sees" the last subsystem. This is true even when overlapping is used. Hence we may expect at least 10 iterations (initial overhead) before we see convergence of WR. In DIRM, the entire system is always being simulated, albeit in a partially reduced form. Hence we do not expect this adverse effect. In order to test this hypothesis we considered the system with $\nu = 0.1, a = 1$, and $b = 0$. This gives rise to a system with diffusion as well as convection propagating towards the decreasing s direction ($a > 0$). This can be seen from Figure 5.5, where the initial condition as well as the solution (benchmark solver) at $t = 5$ are shown. This may be thought of as the initial triangle diffusing and propagating to the left at the same time. Thus there is more "information flow" from right to left than from left to right. In order to capture the waveform for the first subsystem (the leftmost 10 grid points) accurately we need to capture the information flow from the other subsystems. Hence we could expect that the WR method would take at least 10 iterations for convergence and also expect it to converge slower for the first (leftmost) subsystem than for the last (rightmost) subsystem. We picked a simulation interval $[0, 10]$ so that the entire system decayed to zero. We found that WR did not converge even after 30 iterations, and hence used overlapping by three variables, keeping the number of subsystems the

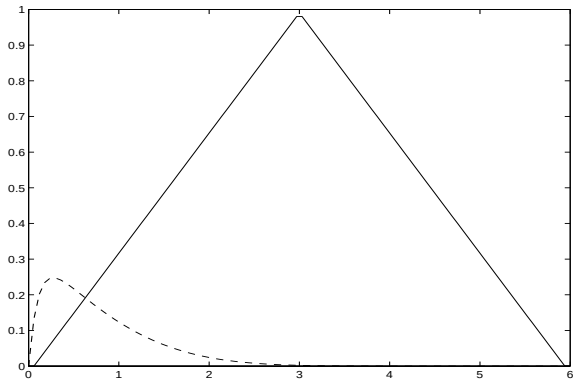

FIG. 5.5. *Plot of the benchmark solution $x(t,s)$ versus s at time $t=0$ (solid) and at time $t=5$ (dashed) for the convection-diffusion case with $\nu=0.1, a=1, b=0$.*

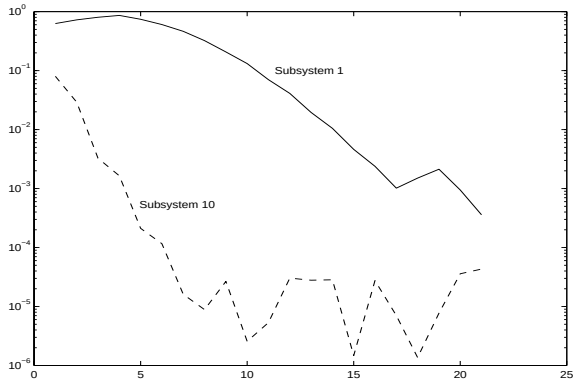

FIG. 5.6. *Convergence of subsystems 1 and 10 for WR with overlap $o=3$ for the convection-diffusion case with $\nu=0.1, a=1, b=0$. Plot of the difference $\sup\{\|x_i^{(j)}(t)-x_i^{(j-1)}(t)\|_2 : t\in[0,T]\}$ between successive iterates versus the iteration step j for subsystems $i=1$ and $i=10$.*

same. This resulted in the first nine subsystems being of size 13 and the last one being of size 10. The convergence plots for the overlapped WR for the first and last subsystems are shown in Figure 5.6, which confirms our intuition. The DIRM method did not experience this overhead and converged in three iterations. Figures 5.7 and 5.8 compare the convergence rates and Figure 5.9 compares the subsystem errors for DIRM and WR.

Second, we considered the system with $\nu=0.1, a=6$, and $b=6$. This system has a dominant reactive term. We picked the simulation interval $[0,1.2]$ in which the system had an explosive reaction after which it decayed to zero. The benchmark simulation showed that subsystem 1 (leftmost) underwent the most explosive change; see Figure 5.10. DIRM and WR with overlapping ($o=3$) performed comparably. Even though the maximum error (Table 5.2) seems large for both DIRM and WR with overlap, it occurred in subsystem 1 (which underwent the most explosive growth), and it is small compared to the peak value of the subsystem trajectory. In fact it was hard to visually distinguish the trajectory plots of subsystem 1 for DIRM and overlapped WR from those of the benchmark solution in Figure 5.10.

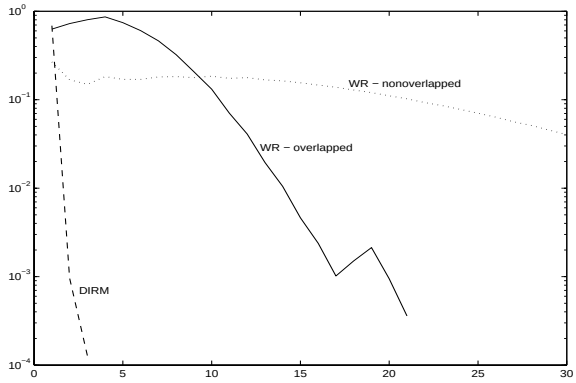

FIG. 5.7. *Convergence of subsystem* 1 *for WR with overlap* $o = 3$*, WR without overlap, and DIRM for the convection-diffusion case with* $\nu = 0.1, a = 1, b = 0$*. Plot of the difference* $\sup\{\|x_i^{(j)}(t) - x_i^{(j-1)}(t)\|_2 : t \in [0,T]\}$ *between successive iterates versus the iteration step* j *for the subsystem* $i = 1$*.*

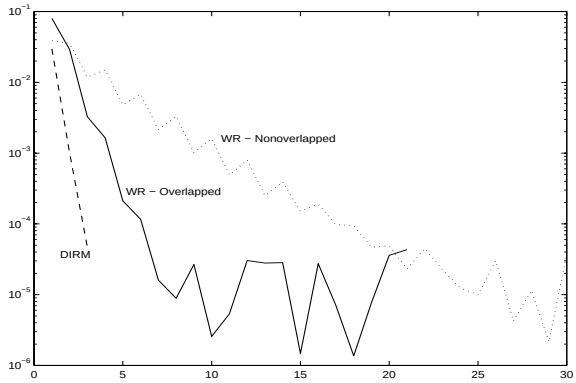

FIG. 5.8. *Convergence of subsystem* 10 *for WR with overlap* $o = 3$*, WR without overlap, and DIRM for the convection-diffusion case with* $\nu = 0.1, a = 1, b = 0$*. Plot of the difference* $\sup\{\|x_i^{(j)}(t) - x_i^{(j-1)}(t)\|_2 : t \in [0,T]\}$ *between successive iterates versus the iteration step* j *for the subsystem* $i = 10$*.*

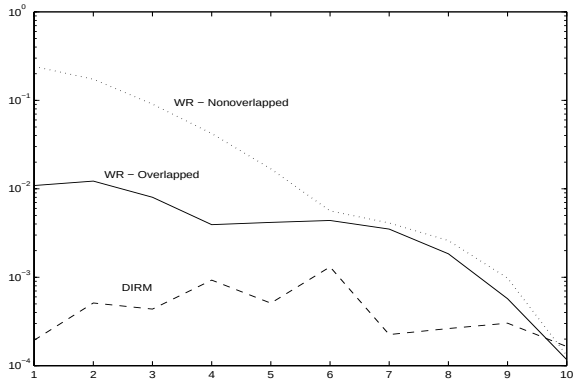

FIG. 5.9. *Errors of each subsystem for WR with overlap* $o = 3$*, WR without overlap, and DIRM for the convection-diffusion case with* $\nu = 0.1, a = 1, b = 0$*. Plot of the error in* i*th subsystem given by* $\sup\{\|\hat{x}_i(t) - x_i(t)\|_2 : t \in [0,T]\}$*, where* $\hat{x}_i$ *is the iterative method solution and* x_i *is the benchmark solution versus the subsystem* i*.*

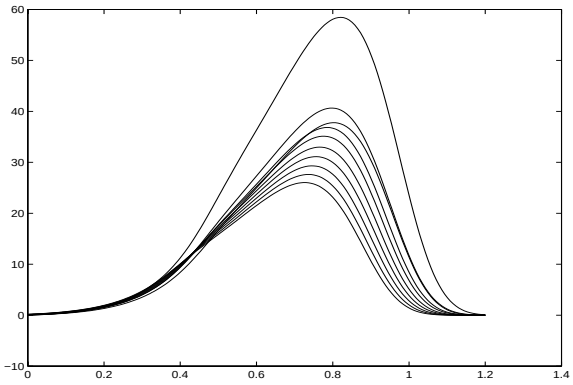

FIG. 5.10. *Plot of the benchmark solution of all* 10 *of the states of subsystem* 1 *for the reaction-convection-diffusion case with* $\nu = 0.1, a = 6, b = 6$.

Finally, we simulated the purely diffusive system with $\nu = 0.1, a = 0$, and $b = 0$. In this case WR performed worst, and DIRM performed best, showing a very clear advantage over WR. Overlapping by $o = 3$ was not sufficient to achieve convergence of WR. However, a bigger overlap of $o = 5$ achieved convergence.

In summary, DIRM seems to converge better than WR for both the convection-diffusion and pure diffusion cases, with the pure diffusion case being the strongest point for DIRM. For the reaction-convection-diffusion case there is no clear winner. Since the error in the POD method is large when system trajectories undergo explosive growth in the interval of interest ([13]), it is not surprising that DIRM performed worst for this type of equation. In contrast, WR seems to have performed best for the reaction-convection-diffusion case.

5.3. Example: Almost coincident eigenvalues $\lambda_k \approx \lambda_{k+1}$ and the modified DIRM method. The convergence analysis of DIRM in section 4.6 predicts difficulties in convergence if the eigenvalues λ_k and λ_{k+1} of the covariance matrix of the fixed point trajectory of any subsystem are very close. To generate such an example, we employ the equation

$$\dot{x} = A(x - f(t)) + f'(t), \tag{5.6}$$

which for any choice of A has $x = f(t)$ as the solution corresponding to the initial condition $x(0) = f(0)$.

Consider the following trajectory $g(t) \in \mathbb{R}^3$ such that the covariance matrix for the interval $[0, 1]$ has prescribed eigenvalues λ_1, λ_2, and λ_3:

$$g(t) = \left(\sqrt{2\lambda_1}\sin(2\pi t), \sqrt{2\lambda_2}\cos(2\pi t), \sqrt{2\lambda_3}\sin(4\pi t)\right).$$

Note that $g(0) = (0, \sqrt{2\lambda_2}, 0)$. We may construct a system of the form (5.6) which is six dimensional, and when split into two subsystems (each of dimension 3) the subsystem solution trajectories are both $g(t)$. According to the analysis of section 4.5, if A is diagonally dominant, and its fundamental modes do not grow substantially in the interval of simulation $[0, 1]$, and the POD projection error is small, then we

expect the fixed point trajectories of the subsystems to be close to the true solution $g(t)$. Thus for the system in (5.6), if we set $f(t) = (g(t), g(t))$, $\lambda_3 = \lambda_2$, and choose an A with the above properties and the initial condition $x(0) = (0, \sqrt{2\lambda_2}, 0, 0, \sqrt{2\lambda_2}, 0)$, then we can expect difficulties in convergence.

Numerical experiments were conducted with A obtained from discretizing the PDE in section 5.2 with $\nu = 1$, $a = b = 0$, and six interior points. The choice of $\lambda_1 = 0.5, \lambda_2 = \lambda_3 = 0.2$ lead to eight iterations for convergence; the choice of $\lambda_1 = 0.5, \lambda_2 = 0.2, \lambda_3 = 0.199$ required 12 iterations; and the choice $\lambda_1 = 0.5, \lambda_2, \lambda_3 = 0.19$ converged in four iterations. In other cases, where λ_2 and λ_3 were further separated, convergence took a similar number of (five or less) iterations.

Remark 5.1. Note that the $\lambda_2 = 0.2, \lambda_3 = 0.19$ case was worse than the $\lambda_2 = \lambda_3 = 0.2$ case because the fixed point trajectory is slightly different from the true solution trajectory. As a verification of our analysis we computed the quantities $\mathcal{C}_1$ and $\mathcal{C}_2$ of equations (4.30) for the fixed point trajectories of the above examples and observed that the larger they were the more the iterations needed for convergence.

In order to make DIRM robust against such situations we tried the following "modified DIRM" method. In modified DIRM, reduced models are computed from a covariance matrix and mean value that are a weighted combination of the covariance matrix and mean value of the current trajectory and some precomputed covariance matrix and mean which are typically obtained from an ensemble of trajectories such as those with initial conditions uniformly chosen from the unit sphere. Thus at the αth iteration, given trajectory $x^{(\alpha)}$ of a subsystem we compute the mean $\bar{x}^{(\alpha)}$ and the covariance matrix $R^{(\alpha)}$ of that trajectory as usual. However, instead of using $\bar{x}^{(\alpha)}$ and $R^{(\alpha)}$ to obtain the reduced model we compute

$$\tilde{R}^{(\alpha)} = \beta R^{(\alpha)} + (1-\beta) R_0,$$
$$\tilde{\bar{x}}^{(\alpha)} = \beta \bar{x}^{(\alpha)} + (1-\beta)\bar{x}_0,$$

where $0 < \beta \leq 1$, and then compute the projection $\tilde{P}^{(\alpha)}$ corresponding to $\tilde{R}^{(\alpha)}$. The new reduced model is given by $\tilde{\bar{x}}^{(\alpha)}$ and $\tilde{P}^{(\alpha)}$.

Here R_0 and $\bar{x}_0$ are precomputed from some ensemble of trajectories with various initial conditions and do not change from iteration to iteration. This method changes the fixed point of DIRM. Typically if β is small you would expect the method not to be so accurate.

When we applied the modified DIRM with $\beta = 0.9$, for the worst case above ($\lambda_1 = 0.5, \lambda_2 = 0.2, \lambda_3 = 0.199$), we converged in four iterations, with more or less the same accuracy as the unmodified DIRM. It is important to note that the precomputed covariance matrix R_0 should have reasonable separation between its kth and $k+1$st eigenvalues. Then for sufficiently small β we are guaranteed to have sufficient separation of λ_k and λ_{k+1}, the eigenvalues of $\tilde{R}$. This example confirms our analysis, and the modified DIRM method provides a safeguard against the situation of coincident eigenvalues.

Remark 5.2. In the modified DIRM method, it is easy to see that when $\beta = 0$ we have immediate convergence, since the reduced models do not change. However, its accuracy is not as good as that of the regular DIRM method. When $\beta = 1$ we have the regular DIRM method, which is more accurate, but does not always have good convergence behavior. So one may expect that by choosing an appropriate β we could achieve a good compromise between convergence and accuracy. However, the numerical experiments with the PDE example of section 5.2 showed that the convergence rate did not depend monotonically on β. For the parameter values

($\nu = 0.1, a = 6, b = 6$), subsystem reduced model dimension $k = 2$, and the time interval $[0, 0.5]$, convergence took 12 iterations for $\beta = 1$, 10 iterations for $\beta = 0.8$, 13 iterations for $\beta = 0.5$, and for the $\beta = 0$ case 1 iteration (as expected). This could be because there is an intermediate regime of β values where the loss of accuracy affects the convergence negatively. It should be noted that the WR method took more than 15 iterations.

5.4. Example: Fixed point trajectory with zero POD projection error. For the example in section 5.3, if we choose $\lambda_1 = 0.5, \lambda_2 = 0.2$, and $\lambda_3 = 0$, we have a solution trajectory which has zero POD projection error. The fixed point trajectory being close to the true solution also had almost zero POD projection error. Yet DIRM took four iterations to converge, in agreement with the convergence analysis (see section 4.6).

When trajectories of all the subsystems always lie in a k dimensional subspace (where k is the dimension of all the reduced order models), the POD projection error is always zero, and in this case convergence is immediate (in agreement with the convergence analysis). This can be numerically observed from an example $\dot{x} = Ax$, where rows of A corresponding to each subsystem are of rank k or less. When the row rank is strictly less than k we have zero POD projection error as well as coincident eigenvalues ($\lambda_k = \lambda_{k+1} = 0$). In this case DIRM still converges immediately, even though the projection matrices computed at each step may not converge.

6. Conclusions and future work. We have presented a new dynamic iteration called DIRM for simulation of large scale interconnected systems. DIRM uses reduced order models (obtained here via POD) of subsystems which are also refined during the iterations. We provided an analysis of the DIRM method as applied to linear time invariant systems of ODEs consisting of two subsystems, giving results on accuracy and convergence of DIRM. We also presented numerical examples, including some special cases chosen to test the validity of the analysis and to illustrate some special situations, and two realistic examples: a nonlinear power grid model and a discretized linear reaction-convection-diffusion type PDE in one dimension. Both the power grid and the PDE examples demonstrated the success of DIRM. In the PDE example we also provided comparisons with WR. This example showed that DIRM has clear advantages over WR for pure diffusion and convection-diffusion-type equations. DIRM performed worst for systems showing explosive reactions, for which WR performed best.

Future work will include DAEs as well as hybrid systems such as the power grid with failure models resulting in discontinuous changes in system parameters. The complementary nature of DIRM and WR seen in the PDE example suggests that the development of an approach that combines the two methods in an optimal manner might prove valuable in parallel computation of large scale systems. The framework of DIRM allows for the use of model reduction techniques other than POD provided that they are data driven. Since the POD reduced models may not achieve considerable savings for nonlinear banded Jacobian systems [13], it might be advantageous to explore the use of other model reduction methods.

Acknowledgments. We would like to thank John C. Doyle for suggesting the general notion of iterating reduced order models of subsystems. We would also like to thank Pablo Parrilo for providing us with the software for the power grid generation.

REFERENCES

[1] Y. Cao and L. Petzold, *A Note on Model Reduction for Analysis of Cascading Failures in Power Systems*, manuscript.

[2] M. Gander, *A waveform relaxation algorithm with overlapping splitting for reaction diffusion equations*, Numer. Linear Algebra Appl., 6 (1999), pp. 125–145.

[3] S. Glavaski, J. Marsden, and R. Murray, *Model reduction, centering, and the Karhunen-Loève expansion*, in Proceedings of the IEEE Control and Decision Conference, Tampa, FL, 1998, pp. 2071–2076.

[4] G. Golub and C. Van Loan, *Matrix Computations*, Johns Hopkins University Press, Baltimore, London, 1996.

[5] P. Holmes, J. Lumley, and G. Berkooz, *Turbulence, Coherent Structures, Dynamical Systems and Symmetry*, Cambridge University Press, Cambridge, UK, 1996.

[6] S. Lall, J. Marsden, and S. Glavaski, *Empirical model reduction of controlled nonlinear systems*, in Proceedings of the 14th IFAC World Congress, Beijing, People's Republic of China, 1999, pp. 473–478.

[7] E. Lelarasmee, A. Ruehli, and A. Sangiovanni-Vincentelli, *The waveform relaxation method for time-domain analysis of large scale integrated circuits*, IEEE Transactions on Computer-Aided Design of Integrated Circuits and Systems, 1 (1982), pp. 131–145.

[8] U. Miekkala, *Remarks on waveform relaxation method with overlapping splittings*, J. Comput. Appl. Math., 88 (1997), pp. 349–361.

[9] U. Miekkala and O. Nevanlinna, *Quasinilpotency of the operators in Picard-Lindelöf iteration*, Numer. Funct. Anal. Optim., 13 (1992), pp. 203–221.

[10] B. Moore, *Principal component analysis in linear systems: Controllability, observability, and model reduction*, IEEE Trans. Automat. Control, 26 (1981), pp. 17–31.

[11] P. Parrilo, F. Paganini, G. Verghese, B. Lesieutre, and J. Marsden, *Model reduction for analysis of cascading failures in power systems*, in Proceedings of the American Control Conference, San Diego, CA, 1999, pp. 4028–4212.

[12] I. Pérez-Arriaga, G. Verghese, F. Pagola, J. Sancha, and F. Schweppe, *Developments in selective modal analysis of small-signal stability in electric power systems*, Automatica, 26 (1990), pp. 215–231.

[13] M. Rathinam and L. Petzold, *A new look at proper orthogonal decomposition,* SIAM J. Numer. Anal., submitted.

[14] M. Rathinam and L. Petzold, *An iterative method for simulation of large scale modular systems using reduced order models*, in Proceedings of the IEEE Control and Decision Conference, Sydney, Australia, 2000.

[15] K. Zhou and J. Doyle, *Essentials of Robust Control*, Prentice-Hall, Englewood Cliffs, NJ, 1998.